Anal. Chem. **2000,** *72,* 1894−1904

Phosphorescent Oxygen Sensors Utilizing Sulfur−Nitrogen−Phosphorus Polymer Matrixes: Synthesis, Characterization, and Evaluation of Poly(thionylphosphazene)-*b*-Poly(tetrahydrofuran) Block Copolymers

Ralph Ruffolo,[†] Christopher E. B. Evans,[†] Xiao-Hua Liu,[†] Yizeng Ni,[†] Zhen Pang,[†] Peter Park,[†] Andrew R. McWilliams,[†] Xijia Gu,[‡] Xin Lu,[†] Ahmad Yekta,[†,§] Mitchell A. Winnik,*[,†] and Ian Manners*[,†]

Department of Chemistry, University of Toronto, 80 St. George Street, Toronto, M5S 3H6, Ontario, Canada, and Photonics Research Ontario, University of Toronto, 60 St. George Street, Toronto, M5S 1A7, Ontario, Canada

We examine the use of thionylphosphazene-based block copolymers as matrixes for oxygen sensor applications. Poly(aminothionylphosphazene)-*b*-poly(tetrahydrofuran) ($PATP_y$−$PTHF_x$) block copolymers were prepared via reaction of ring-opened poly(chlorothionylphosphazene) with THF and subsequently with excess *n*-butylamine (to form $PBATP_y$−$PTHF_x$) or methylamine (to form $PMATP_y$−$PTHF_x$). The block copolymers were characterized by NMR, gel permeation chromatography, and differential scanning calorimetry. Films of $PBATP_y$−$PTHF_x$ block copolymers containing platinum octaethylporphyrin or $[Ru(dpp)_3]Cl_2$ (dpp = 4,7-diphenyl-1,10-phenanthroline) as the oxygen-sensitive chromophore were prepared, and time-scan experiments were carried out to determine the diffusion coefficients, D_{O_2}, and solubilities, S_{O_2}, of oxygen therein. Despite microphase separation, the data fit well to a simple Fick's law description of oxygen diffusion and gave D_{O_2} values smaller than that for the *n*-butylamino-substituted $PBATP_{635}$. For films freshly annealed above the melting point of $PTHF_x$, the D_{O_2} values were 35−50% (dye-dependent) larger than after aging 3 days at room temperature. Films with $[Ru(dpp)_3]Cl_2$ as the dye were evaluated as media for phosphorescent pressure-sensing. The dye-containing polymer films exhibit linear Stern−Volmer-like plots, even at high dye concentrations, as well as good photostability, and significantly higher sensitivity to oxygen quenching than simple mixtures of the analogous homopolymers.

The design of polymeric materials for the construction of sensing devices is an area of intense current interest.[1−3] Phosphorescent sensors consisting of transition metal complexes immobilized in polymer matrixes have attracted attention as oxygen sensors for both biomedical and barometric applications.[4−8] Such systems typically incorporate dyes with oxygen-quenchable excited states, such as platinum octaethylporphyrin (PtOEP) or ruthenium(II) polypyridine complexes, which are dissolved or dispersed in a polymer matrix.[4−8] The matrix material requires high oxygen permeability and must be chemically robust with respect to singlet oxygen, which is a byproduct of the quenching process. Inorganic polymers with outstanding O_2-permeability and thermooxidative stability, such as polysiloxanes, have attracted significant attention. Polysiloxanes, however, generally must be cross-linked (cured) after solution processing in order to obtain dimensional stability.[4−8] To obtain a fundamental understanding of the factors that influence the performance of pressure sensing matrixes, tunable and structurally well-defined polymers are required to allow structure−function relationships to be established.

In a previous communication we reported that a poly(thionylphosphazene) (PTP) with *n*-butylamino substituents, $PBATP_y$ (where *y* represents the degree of polymerization), provides an excellent polymer matrix for phosphorescent oxygen sensor applications.[9] In particular, cross-linking is unnecessary for

* To whom correspondence should be addressed. E-mail addresses. mwinnik@chem.utoronto.ca; imanners@chem.utoronto.ca.

† Department of Chemistry.

‡ Photonics Research Ontario.

§ Permanent address: Imaging Research Inc., 500 Glenridge Ave., St. Catherines, ON, Canada L2S 3A1.

(1) (a) Swager, T. M.; Marsella, M. J. *Adv. Mater.* **1994**, *6*, 595. (b) Zhou, Q.; Swager, T. M. *J. Am. Chem. Soc.* **1995**, *117*, 7017. (c) *Fluorescent Chemosensors for Ion and Molecular Recognition;* Czarnik, A. W., Ed.; ACS Symposium Series 538, American Chemical Society: Washington, DC 1993. (d) Bäuerle, P.; Scheib, S. *Adv. Mater.* **1993**, *5*, 848. (e) Bartlett, P. N.; Birkin, P. R. *Synth. Met.* **1993**, *61*, 15.

(2) (a) Klimant, I.; Wolfbeis, O. S. *Anal. Chem.* **1995**, *67*, 3160. (b) Demas, J. N.; DeGraff, B. A. J. *Chem. Educ.* **1997**, *74*, 690.

(3) Dorn, R.; Baums, D.; Kersten, P.; Regener, R. *Adv. Mater.* **1992**, *4*, 464.

(4) Li X. M.; Ruan, F. C.; Wong, K. Y. *Analyst* **1993**, *118*, 289.

(5) (a) Preininger, C.; Klimant, I.; Wolfbeis, O. S. *Anal. Chem.* **1994**, *66*, 1841. (b) Di Marco, G.; Lanza, M.; Campagna, S. *Adv. Mater.* **1995**, *7*, 468. (c) Moreno Bondi, M. C.; Wolfbeis, O. S.; Leiner, M. J. P.; Schaffar, B. P. H. *Anal. Chem.* **1990**, *62*, 2377.

(6) Kavandi, J.; Callis, J.; Gouterman, M.; Khalil, G.; Wright, D.; Green, E.; Burns, D.; McLachlan, B. *Rev. Sci. Instrum.* **1990**, *61*, 3341.

(7) (a) Bacon, J. R.; Demas, J. N. *Anal. Chem.* **1987**, *59*, 2780. (b) Demas, J. N.; De Graff, B. A. *Anal. Chem.* **1991**, *63*, 829A.

(8) Carraway, E. R.; Demas, J. N.; DeGraff, B. A.; Bacon, J. R. *Anal. Chem.* **1991**, *63*, 337.

(9) Pang, Z.; Gu, X.; Yekta, A.; Masoumi, Z.; Coll, J. B.; Winnik, M. A.; Manners, I. *Adv. Mater.* **1996**, *8*, 768.

10.1021/ac9909610 CCC: $19.00
Published on Web 03/17/2000

dimensional stability and this gives rise to the additional advantage that the sensing layer can be recycled after use by dissolution in common organic solvents.[10] Unfortunately $PBATP_y$, an amorphous material with a T_g of −17 °C, forms rather tacky films which, although useful for fundamental studies, are unsuitable for many applications.[9] The visualization of air flow over objects such as aircraft, for example, requires a material that provides a smooth, abrasion-resistant surface so that the sensing process is nonintrusive. In this paper we describe a step toward a resolution of this problem through modification of $PBATP_y$ with poly(tetrahydrofuran) ($PTHF_x$) resulting in block copolymers of composition $PBATP_y$−$PTHF_x$ (where x is the degree of polymerization of THF).

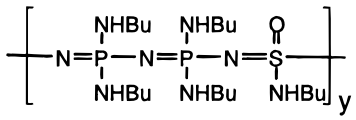

$PBATP_y$

EXPERIMENTAL SECTION

Materials. Polymers were synthesized under nitrogen atmosphere either in an Innovative Technology glovebox or by standard Schlenk line techniques. Solvents were dried according to standard methods.[11] $PTHF_x$ was prepared according to literature procedures using trimethylsilyl triflate as the initiator at −10 °C (M_w = 8.14 × 10^4, PDI = 1.6).[25] Cyclic thionylphosphazene ($NSOCl(NPCl_2)_2$),[12] the corresponding ring-opened polymer $PCTP_y$,[20] the methyl-substituted polymer $PMATP_y$ (M_w = 5.0 × 10^3, PDI = 1.5),[20] and the butyl-substituted polymer $PBATP_y$ (M_w = 3.69 × 10^5, PDI = 1.8)[9] were all prepared according to literature methods. 1,1,1-Trichloroethane (ACS) was purchased from Aldrich and used as received. $[Ru(dpp)_3]Cl_2$ was synthesized according to the procedure described by Lin et al.[13] PtOEP was purchased from Porphyrin Products, Inc. and used as received.

$^{31}P\{^1H\}$ NMR spectra were recorded on a Varian XL-300 spectrometer ^1H and ^{13}C NMR spectra on a Varian XR-200 spectrometer operating at 200.0 and 50.3 MHz, respectively. Chemical shifts are reported relative to $SiMe_4$ (^1H or ^{13}C) or to external (85%) H_3PO_4. Molecular weights were estimated by gel permeation chromatography (GPC) using a Waters Associates liquid chromatograph equipped with a 510 HPLC pump, U6K injector, Ultrastyragel columns with a pore size of 10^3 and 10^5 Å, and a Waters 410 differential refractometer. A flow rate of 1.0 mL/min was used, and samples were dissolved in a solution of 0.1% tetra-*n*-butylammonium bromide in THF. Polystyrene standards were used for calibration purposes. The DSC thermograms were calibrated with the melting transitions of *n*-heptane and decane were obtained at a heating rate of 10 °C/min.

Synthesis of Polymers. Poly(butylaminothionylphosphazene)-*b*-Poly(tetrahydrofuran), $PBATP_y$−$PTHF_x$. $NSOCl(NPCl_2)_2$ (2.0 g) was heated in a sealed, evacuated Pyrex tube at 165 °C for 4 h. The tube contents were dissolved in ∼ 40 mL of CH_2Cl_2, and the solution was then concentrated to ∼10 mL and added dropwise to 200 mL of stirred hexanes via cannula. The colorless, moisture-sensitive, elastomeric polymer $PCTP_y$ was dissolved in 100 mL of THF and the solution then stored in the refrigerator at −14 °C for 48 h. A significant increase in solution viscosity was noticed. *n*-Butylamine was then added dropwise to the polymer solution at 0 °C and allowed to stir for 24 h. The crude product was obtained by dropwise addition of the concentrated solution to water and was purified twice by precipitation of THF solutions into water and subsequently three times by precipitating CH_2Cl_2 solutions into hexanes. The purified product was dried under high vacuum for 24 h at ambient temperature; yield of $PBATP_y$−$PTHF_x$, a colorless film-forming material, 1.34 g (84%). ^{31}P NMR (CH_2Cl_2) δ (ppm): 2.05, 1.81. ^1H NMR ($CDCl_3$) δ (ppm): 3.38 (s, br, THF_x), 3.04 (m, br, NH), 2.84 (m, br, Bu), 1.57 (m, br, THF_x), 1.46 (m, br, Bu), 1.36 (m, br, Bu), 0.91 (m, br, Bu-*CH*$_3$). ^{13}C NMR (CD_2Cl_2) δ (ppm): 70.9 (THF_x), 41.1 (Bu), 34.3 (Bu), 27.0 (THF_x), 20.7 (Bu), 14.2 (Bu). DSC: T_g = −70 °C and T_m = 40 °C for the $PTHF_x$ block, T_g = −16 °C for the $PBATP_y$. GPC: $PBATP_{705}$−$PTHF_{1300}$, M_w = 3.05 × 10^5, PDI = 1.9; $PBATP_{280}$−$PTHF_{2740}$, M_w = 2.16 × 10^5, PDI = 1.5; $PBATP_{135}$−$PTHF_{4925}$, M_w = 2.36 × 10^5, PDI = 1.9.

Poly(methylaminothionylphosphazene)-*b*-Poly(tetrahydrofuran), $PMATP_y$−$PTHF_x$. Pure $PCTP_y$ (0.43 g) was dissolved in 20 mL of THF, and the resulting solution was stored at −14 °C for 48 h, resulting in a significant increase in viscosity. The solution was was diluted with 100 mL of CH_2Cl_2, and predried methylamine gas was introduced at 0 °C, resulting in the immediate formation of a white precipitate. The reaction mixture became clear after ∼5 min at which time methylamine flow was resumed for a further 5 min. The solution was warmed to ambient temperature over 2 h, was concentrated to ∼20 mL, and was filtered through a glass frit. Purification was carried out by precipitating THF solutions (∼10 mL) into water three times and subsequently precipitating CH_2Cl_2 solutions into hexanes three times. Final product was dried under high vacuum for 24 h at ambient temperature. Yield of $PMATP_y$−$PTHF_x$, a colorless film-forming material, was 0.28 g (89%). ^{31}P NMR (CH_2Cl_2) δ (ppm): 5.10. ^1H NMR ($CDCl_3$) δ (ppm): 5.51 (m, br SN*H*), 3.38 (s, br, THF_x), 3.04 (m, br, PN*H*), 2.72 (m, br, SNC*H*$_3$), 2.51 (s, br, PNC*H*$_3$), 1.57 (m, br, THF_x). ^{13}C

(10) Yekta, A.; Masoumi, Z.; Winnik, M. A. *Can. J. Chem.* **1995**, *73*, 2021.
(11) Perrin, D. D.; Armarego, W. L. F. *Purification of Laboratory Chemicals*, 3rd ed.; Pergamon Press: New York, 1988.
(12) Baalmann, H. H.; Velvis, H. P.; van de Grampel, J. C. *Recl. Trav. Chim. Pays-Bas* **1972**, *91*, 935.
(13) Lin, C.-T.; Böttcher, W.; Chow, M.; Crentz, C.; Sutin, N. *J. Am. Chem. Soc.* **1976**, *98*, 6536.
(14) Masoumi, Z.; Stoeva, V.; Yekta, A.; Winnik, M. A.; Manners, I. In *Polymers and Organic Solids, Studies of Oxygen Diffusion in Polysiloxane Resins with Application to Luminescence Barometry*; Shi, L., Zhu, D., Eds.; Science Press: Beijing, China, 1997; pp 157−168.
(15) Masoumi, Z.; Stoeva, V.; Yekta, A.; Pang, Z.; Manners, I.; Winnik, M. A. *Chem. Phy. Lett.* **1996**, *261*, 551.
(16) For a review, see: Lu, X.; Winnik, M. A. In *Organic, Physical, and Materials Photochemistry*, Ramamurthy, V., Schanze, K. S., Eds.; Marcel Dekker: New York, 2000; Vol. 5 of *Molecular and Supramolecular Photochemistry*.
(17) (a) Mills, A.; Thomas, M. *Analyst* **1997**, *122*, 63. (b) Mills, A.; Chang, Q. *Analyst* **1992**, *117*, 1461.
(18) (a) Roy, A. K.; Burns, G. T.; Lie, G. C.; Grigoras, S. *J. Am. Chem. Soc.* **1993**, *115*, 2604. (b) Roy, A. K. *J. Am. Chem. Soc.* **1992**, *114*, 1530.
(19) (a) Allcock, H. R. *J. Inorg. Organomet. Polym.* **1992**, *2*, 197. (b) Allcock, H. R. *Chem. Mater.* **1994**, *6*, 106. (c) Allcock, H. R. *Adv. Mater.* **1994**, *6*, 106.
(20) Ni, Y.; Park, P.; Liang, M.; Massey, J.; Waddling, C.; Manners, I. *Macromolecules* **1996**, *29*, 3401.
(21) Gates, D. P.; Edwards, M.; Liable-Sands, L. M.; Rheingold, A. L.; Manners, I. *J. Am. Chem. Soc.* **1998**, *120*, 3249.
(22) Allcock, H. R.; Kugel, R. L. *J. Am. Chem. Soc.* **1965**, *87*, 4216.
(23) Manners, I. *Coord. Chem. Rev.* **1994**, *137*, 109.
(24) Ni, Y. Ph.D. Thesis, University of Toronto, 1993.
(25) Dreyfuss, P. *Poly(tetrahydrofuran)*; Gordon and Breach Science Publishers: New York, 1982.

Table 1. Permeation Properties of Oxygen in Polymer Films Containing PtOEP or $[Ru(dpp)_3]Cl_2$ as the Oxygen-Sensitive Luminophore, Calculated from Time-Scan Experiments

polymer[a]	D_{O_2}, $\times 10^{-6}$ $cm^2 \cdot s^{-1}$	S_{O_2}, $\times 10^{-4}$ $M \cdot atm^{-1}$	$P_{O_2} = D_{O_2}S_{O_2}$, $\times 10^{-12}$ $mol \cdot cm^{-1} \cdot s^{-1} \cdot atm^{-1}$	τ^0, $\times 10^{-6}$ s	B
$PBATP_y$/PtOEP	3.73 ± 0.97	10.3 ± 2.6	3.85 ± 0.20	103 ± 1	59.8 ± 3.1
$PBATP_y/[Ru(dpp)_3]Cl_2$	3.72 ± 0.74	4.89 ± 0.97	1.82 ± 0.07	5.4 ± 0.1	1.74 ± 0.07
$PBATP_{705}$−$PTHF_{1300}$/PtOEP (1 h)	10.9 ± 0.6	0.8 ± 0.1	0.86 ± 0.03	92.0 ± 1.0	12.0 ± 0.6
$PBATP_{135}$−$PTHF_{4925}$/PtOEP (1 h)	1.55 ± 0.07	10.2 ± 0.5	1.58 ± 0.08	96.0 ± 0.5	23.0 ± 1.0
$PBATP_{135}$−$PTHF_{4925}$/PtOEP (3 d)	1.01 ± 0.03	12.0 ± 0.7	1.19 ± 0.03	94.0 ± 0.5	17.4 ± 0.4
$PBATP_{135}$−$PTHF_{4925}/[Ru(dpp)_3]Cl_2$ (1 h)	2.6 ± 0.7	3.7 ± 0.9	1.00 ± 0.06	6.9 ± 0.1	1.05 ± 0.03
$PBATP_{135}$−$PTHF_{4925}/[Ru(dpp)_3]Cl_2$ (3 d)	1.4 ± 0.3	6.7 ± 0.4	0.95 ± 0.06	6.9 ± 0.1[b]	1.00 ± 0.02
$PTHF_x$/PtOEP (1h)	3.2 ± 0.9	7.4 ± 2.1	2.4 ± 0.2	92.1 ± 0.6	33.5 ± 0.9
$PTHF_x$/PtOEP (10 d)	1.0 ± 0.3	19 ± 5	1.9 ± 0.1	86.1 ± 0.7	24.8 ± 3.5
$PTHF_x$/PtOEP (30 d)	0.68 ± 0.17	25 ± 6	1.7 ± 0.1	75.1 ± 0.5	18.9 ± 1.3

[a] The time given in parentheses is the aging time after the samples were removed from the annealing oven. [b] The unquenched lifetime used here is that of the sample 1 h after annealing.

NMR (CD_2Cl_2) δ (ppm): 70.6 (THF_x), 30.3 ($SNCH_3$), 27.0 ($PNCH_3$), 26.5 (THF_x). DSC: $T_g = -79$ °C and $T_m = 34$ °C for the $PTHF_x$ block, $T_g = 13$ °C for $PMATP_y$ block. GPC: $PMATP_y$−$PTHF_x$, $M_w = 1.50 \times 10^5$, PDI = 1.9.

Precipitation Experiment To Show That $PBATP_{135}$-$PTHF_{4925}$ Is Not a Blend. Equivalent precipitation experiments (viscous CH_2Cl_2 solutions into hexanes, with subsequent cooling) were performed upon both a sample of $PBATP_{135}$−$PTHF_{4925}$ and a mechanical blend of $PBATP_{635}$ and $PTHF_{1810}$.

A blend of $PBATP_{635}$ homopolymer (60 mg) and $PTHF_{1810}$ homopolymer (60 mg) was dissolved in CH_2Cl_2 (5 mL) and added dropwise to hexanes (150 mL). The solution was cooled in an ice bath for 30 min, resulting in the precipitation of a white polymer, which was isolated by decanting off the supernatant liquor and was dried in vacuo. Subsequent analysis confirmed the identity of this solid as being 40 mg of $PTHF_{1810}$. ^1H NMR (prior to precipitation) ($CDCl_3$) δ (ppm): 3.40 (s, br, THF_x), 3.04 (m, br, N*H*), 2.86 (m, br, Bu), 1.61 (m, br, THF_x), 1.41 (m, br, Bu), 0.89 (m, br, BuC*H*$_3$). ^1H NMR (after precipitation) ($CDCl_3$) δ (ppm): 3.41 (s, br, THF_x), 1.61 (m, br, THF_x).

A sample of $PBATP_{135}$−$PTHF_{4925}$ was dissolved in CH_2Cl_2 and added dropwise to hexanes. After cooling in ice for 30 min, the resultant solid was collected and dried. Analysis by ^1H NMR confirmed the identity of the precipitate as $PBATP_{135}$−$PTHF_{4925}$. ^1H NMR (prior to precipitation) ($CDCl_3$) δ (ppm): 3.40 (s, 36.7H, THF_x), 2.92 (m, 2.3H, Bu), 1.61 (m, 40.8, THF_x), 1.36 (m, 3.2H, Bu), 0.90 (m, 4.4H, Bu). ^1H NMR (after precipitation) ($CDCl_3$) δ (ppm): 3.40 (s, 35.3H, THF_x), 2.92 (m, 3.5H, Bu), 1.61 (m, 38.6H, THF_x), 1.36 (m, 3.7H, Bu), 0.90 (m, 3.9H, Bu).

Oxygen Diffusion Studies. 1,1,1-Trichloroethane solutions of the polymers under investigation, containing PtOEP or $[Ru(dpp)_3]Cl_2$ dye, were film-cast onto glass substrates via slow evaporation of the solvent at ambient temperatures over ~24 h. The resultant films were annealed at 80 °C in a vacuum oven for ~48 h to remove residual solvent, and the thickness of the films (~0.1 mm) was determined with a micrometer.

The dye-containing films were placed in an optically transparent plastic cuvette fitted with a rubber septum through which gases could be introduced. Films, initially equilibrated with either air or nitrogen, were placed in the sample chamber of a SPEX Fluorolog 2 fluorescence spectrometer equipped with a DMA 3000 data system. The oxygen diffusion coefficients were determined by following the change in phosphorescence emission intensity of the dye in the polymer matrix as a function of time after the inert atmosphere surrounding the film was rapidly replaced by air (O_2 sorption) or after flushing an air-equilibrated sample with a nitrogen atmosphere (O_2 desorption). This method has been shown previously to be suitable for detecting subsecond response times, using GP-197 as the polymeric matrix.[14] Luminescence intensity was monitored in the time-scan mode ($\lambda_{ex} = 535$ nm and $\lambda_{em} = 645$ nm for PtOEP dye, $\lambda_{ex} = 450$ nm and $\lambda_{em} = 610$ for $[Ru(dpp)_3]Cl_2$). In the pulsed laser experiments, dye-containing films were excited by a second harmonic Nd:YAG laser (Spectra Physics DCR3) at 532 nm with a pulse width of ~6 ns. The beam intensity was severely attenuated to prevent sample damage and dye photobleaching. Following sample excitation, the phosphorescence of the polymer films was detected by a Hammamatsu 956 photomultiplier tube connected to a Tektronix model 1912 transient digitizer.

The parameters characterizing oxygen permeability in the various polymers are collected in Table 1.

Luminescence Measurements. 1,1,1-Trichloroethane solutions containing the dye ($[Ru(dpp)_3]Cl_2$) and polymer ($PBATP_y$−$PTHF_x$) were spray coated onto ~2 cm^2 aluminum plates precoated with the acrylic primer Suprime 1 White manufactured by Pratt & Lambert. The dye concentration in the polymer matrixes ranged from 500 to 2500 ppm. Samples were placed in a small pressure chamber controlled using a vacuum pump and compressed air. All measurements were made at ambient temperatures.

The samples were illuminated by a lamp composed of 60 Nichia Single Quantum Well (SQW) 2−3 mW NSPB series blue LEDs with a band maximum at 470 nm and band halfwidth of 20−30 nm. Luminescent light from the sample surface was collected with a camera lens (Nikon Nikkor, 55 mm, 1:1.2) protected by two red filters (Hoya 52 mm R[25A] and Tiffen 52 mm 25 RED 1) and imaged onto a CCD camera (Photometrics CH350) equipped with a cutoff filter (Melles Griot 03FIB004 for $[Ru(dpp)_3]Cl_2$). The pressure of the sample chamber was measured by an analog pressure gauge (model FA 233, Wallace & Tiernan) read to an accuracy of ± 0.05 psi. Evidence for the photostability of the $[Ru(dpp)_3]Cl_2$ dye in one of the polymer matrixes is presented in Table 2.

Table 2. Influence of Exposure Time to Light[a] in the Presence of 0.2 Atm O_2 over a 2 Hour Interval on the Emission Intensity (I) of $[Ru(dpp)_3]Cl_2$ (500 ppm) in $PBATP_{135}$–$PTHF_{4925}$

time (min)	I (at 1 atm)
0	1638 ± 58
60	1616 ± 58
75	1591 ± 52
90	1574 ± 52
120	1525 ± 51

[a] λ_{ex} = 450 nm, intensity = 0.17 mW/cm^2 at the film surface.

DATA AND DATA ANALYSIS

Measuring Oxygen Diffusion via Luminescence Quenching. Diffusion coefficients for oxygen in polymer films were determined by monitoring the time-dependent intensity of dye phosphorescence during both O_2 sorption and desorption experiments (see Experimental Section). Details of such experiments have been published previously and thus only a brief introduction to the underlying theory is provided here.[10,15,16]

Theoretical Considerations. The rate of quencher (oxygen) diffusion into the film can be anticipated to follow Fick's second law:

$$\partial c(x,t)/\partial t = D(\partial^2 c(x,t)/\partial x^2) \tag{1}$$

where $c(x, t)$ is the concentration of the dissolved gas at time t and distance x within the film and D is its diffusion coefficient. A Henry's law dependence between the quencher pressure above the film and the gas concentration in the polymer film is assumed when the quencher concentration in the gas phase is constant. With this approximation, the concentration of quencher oxygen absorbed by the film can be related to exposure time by eq 2.1,

oxygen sorption:

$$Q(x,t) = Q_{eq}\left[1 - \frac{4}{\pi}\sum_{n=\text{odd}}^{\infty}\frac{1}{n}\exp\left(-\frac{n^2\pi^2 Dt}{4L^2}\right)\sin\left(\frac{n\pi x}{2L}\right)\right] \tag{2.1}$$

oxygen desorption:

$$Q(x,t) = Q_{eq}\left[\frac{4}{\pi}\sum_{n=\text{odd}}^{\infty}\frac{1}{n}\exp\left(-\frac{n^2\pi^2 Dt}{4L^2}\right)\sin\left(\frac{n\pi x}{2L}\right)\right] \tag{2.2}$$

first derived by Mills and Chang.[17b] Here $Q(x, t)$ is the concentration of oxygen in a film of thickness L at a depth x and time t. The subscript eq refers to the film in equilibrium with oxygen. That is, Q_{eq} is the equilibrium concentration of oxygen in the film.

During either the O_2 sorption or desorption experiments, the concentration of oxygen in the film changes as a function of time, resulting in a time-dependent emission intensity, $I(t)$. The measured intensity is the sum of the incremental intensities of the dye molecules located at various depths in the film, which in turn are related to $Q(x, t)$. From the Stern–Volmer equation for oxygen quenching, we obtain the expression[10,15]

$$\frac{\partial I^0}{\partial I(x,t)} = 1 + \frac{B}{Q_{eq}}Q(x,t), \quad \partial I^0 = I^0\,\mathrm{d}x/L \tag{3}$$

where the superscript 0 is used here to indicate that no quencher is present in the film. I^0 is, thus, the emission intensity when $Q(x,t) = 0$. B is defined in eq 4. Here σ is the radius of the encounter

$$B = \frac{I^0}{I_{eq}} - 1 = 4\pi\alpha\sigma N_A'\tau^0(D_{O_2}S_{O_2})p_{O_2} = Kp_{O_2} \tag{4}$$

$$K = 4\pi\alpha\sigma N_A'\tau^0(D_{O_2}S_{O_2})$$

complex (~10 Å), α is the probability an encounter complex results in quenching (typically assumed to be one), N_A' is 6.023 × 10^{20} (Avogadro's number divided by 1000), and τ^0 is the lifetime of the dye in the absence of quencher. D_{O_2} and S_{O_2} are the diffusion coefficient and solubility of oxygen in the polymer film, respectively, and p_{O_2} is the pressure of oxygen above the polymer film. In the time-scan experiments described below, p_{O_2} is equal to 0.2 atm. From values of B, one can calculate the permeability ($P_{O_2} = D_{O_2}S_{O_2}$) of oxygen if τ^0 and σ are known. Clearly, the solubility of oxygen in the polymer films can be calculated from P_{O_2} (or B) once D_{O_2} is determined.

To determine values for D_{O_2}, eq 3 must be related to our experimental observable, $I(t)$, which is accomplished using eq 5.

$$I(t) = \frac{I^0}{L}\int_0^L\left[1 + B\frac{Q(x,t)}{Q_{eq}}\right]^{-1}\mathrm{d}x \tag{5}$$

$I(t)$ values calculated using eq 5 are compared with experimental data, using D_{O_2} as the variable for the evaluation of $Q(x,t)$ (see eqs 2). The correct value of D_{O_2} is then taken to be that which results in the best correlation between the experimental and calculated data.

Variable Reference Point Stern–Volmer Plots. If we use p_1 and p_2 to represent two different oxygen pressures, the ratio of the emission intensities of the dye-containing films under these two different pressures, I_1/I_2, is given by eq 6 if the Stern–Volmer

$$\frac{I_1}{I_2} = \frac{1 + Kp_2}{1 + Kp_1} = \frac{1}{1 + Kp_1} + \frac{K}{1 + Kp_1}p_2 \tag{6}$$

equation applies to the system over this pressure range. When p_1 refers to a reference pressure, eq 6 can be rewritten as eq 7 by

$$\frac{I_{ref}}{I_2} = \frac{1}{1 + B} + \frac{B}{1 + B}\left(\frac{p_2}{p_{ref}}\right) \tag{7}$$

considering $B = Kp_{ref}$ and $Kp_2 = Bp_2/p_{ref}$. In the study of air pressure profiles by luminescence barometry, the air pressure P replaces the oxygen pressure p in the above equation. Taking p_{ref} as 1 atm ($P_{1.0}$), the emission intensity (I) at P is related to that ($I_{1.0}$) at 1 atm air pressure, by the expression

$$\frac{I_{1.0}}{I} = \frac{1}{1 + B} + \frac{B}{1 + B}\left(\frac{P}{P_{1.0}}\right) \tag{8}$$

Scheme 1

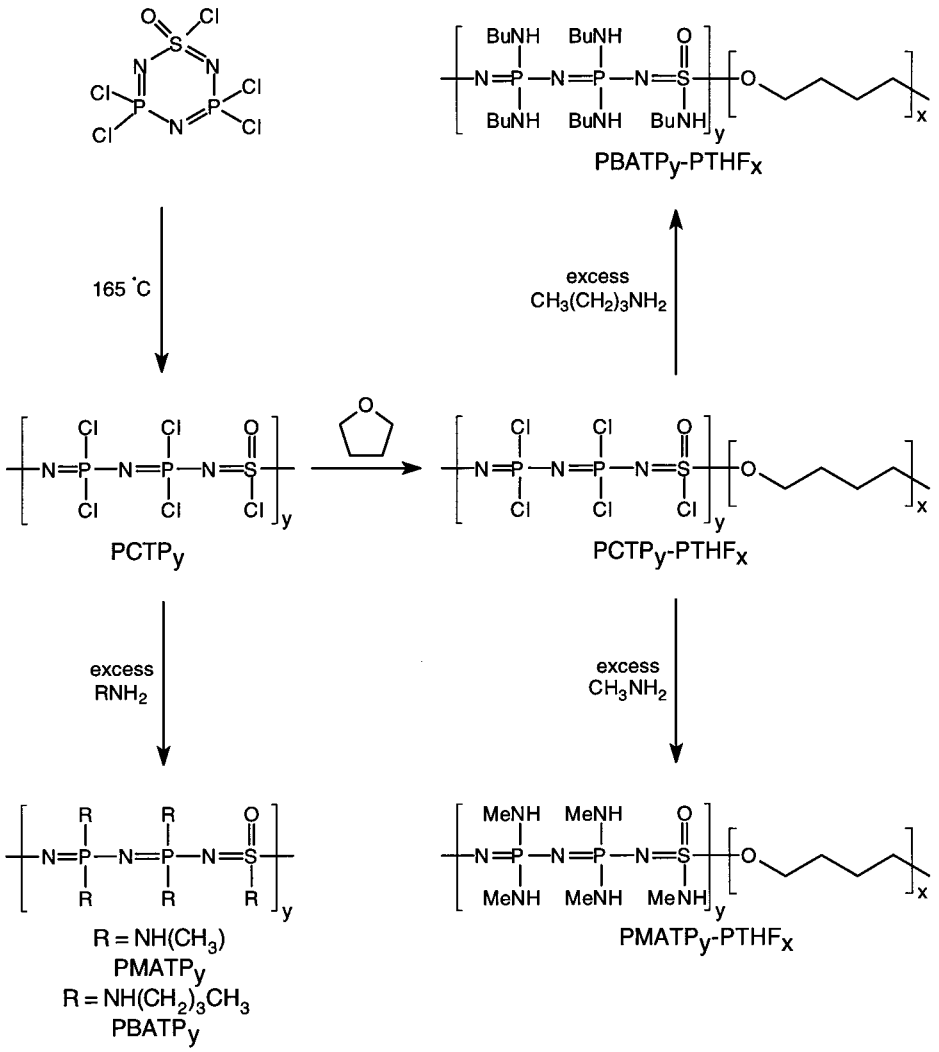

When we fit intensity data as a function of air pressure, we commonly rewrite this expression as

$$I_{1.0}/I = A + Q_S(P/P_{1.0}) \qquad (9)$$

where $Q_S = B/(1 + B)$ is a measure of the sensitivity of the dye−matrix combination to quenching due to a change in air pressure. In this type of experiment, we refer to Q_S as the "quenching sensitivity". We note that while B can take a wide range of values, depending upon the magnitude of $\tau^0 D_{O_2} S_{O_2}$, values of Q_S range from 0 to 1. When $B = 1$, $Q_S = 0.5$, whereas when B is very large, $Q_S \approx 1.0$. It should be clear that Q_S is not equivalent to K_{SV}, the Stern−Volmer constant, which requires the reference point to be the intensity and pressure when the concentration of oxygen is zero.

RESULTS

Synthesis and Characterization of Poly(*n*-butylaminothionylphosphazene)-*b*-Poly(tetrahydrofuran) Block Copolymers. Poly(thionylphosphazenes) are an interesting new class of inorganic polymers with a backbone of sulfur(VI), nitrogen, and phosphorus atoms. These materials can be regarded as hybrids of poly(oxothiazenes) $[S(O)R{=}N]_n$ and polyphosphazenes $[PR_2{=}N]_n$,[18,19] and can be prepared via the ring-opening polymerization (ROP) of the cyclic monomer, $NSOCl(NPCl_2)_2$, either thermally at 165 °C or at ambient temperature in solution with a Lewis acid initiator such as $GaCl_3$.[20,21] In a manner analogous to the preparation of hydrolytically stable poly(organophosphazenes) from $[NPCl_2]_n$,[19,22] the hydrolytically sensitive halogenated polymer $PCTP_y$ can be reacted with nucleophilic reagents to afford hydrolytically stable polymers such as $PBATP_y$.[20] We believe the ROP mechanism involves initiation by a cationic intermediate generated via loss of chloride from the sulfur(VI) center followed by propagation steps in which ring opening of monomer molecules generates a linear polymer with an electrophilic sulfur(VI) center at the chain end.[23]

Dissolution of $PCTP_y$ in PTHF led to an increase in solution viscosity with time. The product of this reaction, $PCTP_y{-}PTHF_x$, is hydrolytically sensitive due to the reactive halogen−element bonds. Hydrolytically stable products were produced by subsequent reactions with primary amines (see Scheme 1) to form the block copolymers $PBATP_y{-}PTHF_x$ (from the reaction with butylamine) and $PMATP_y{-}PTHF_x$ (from the reaction with methylamine). The identity of the products was confirmed by NMR. THF

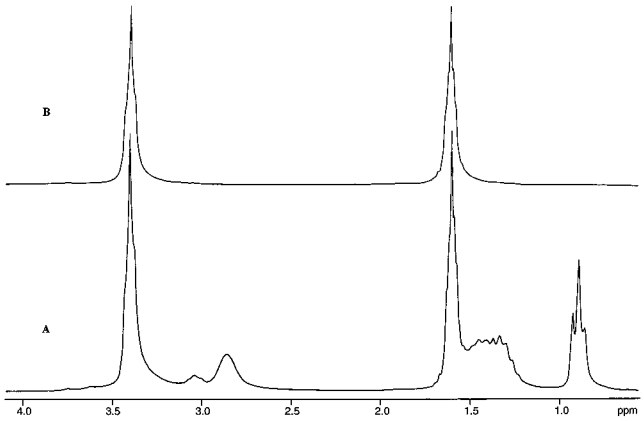

Figure 1. 200 MHz ^{1}H NMR spectra (in $CDCl_3$) of (A) a mechanical blend of $PBATP_y$ and $PTHF_{1810}$ and (B) the product isolated from precipitation into hexanes, $PTHF_{1810}$.

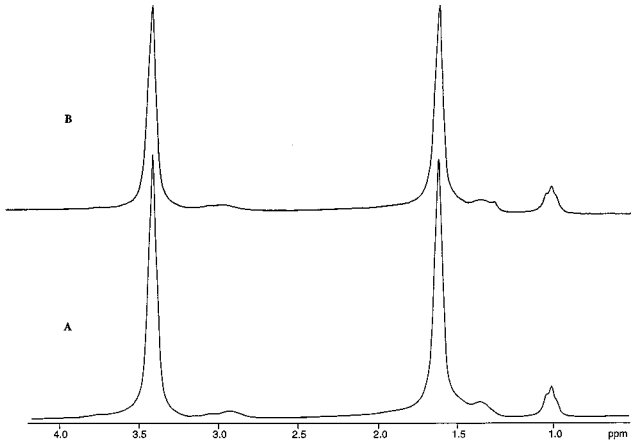

Figure 2. 200 MHz ^{1}H NMR spectra (in $CDCl_3$) of (A) $PBATP_{135}-PTHF_{4925}$ and (B) the product isolated from precipitation into hexanes.

polymerization is believed to be initiated by cationic chain ends of $PCTP_y$.

Characterization of the block copolymers was achieved by ^{1}H, ^{13}C, and ^{31}P NMR, and by GPC. Significantly, the ^{31}P NMR spectra of the block copolymers were identical to those of the corresponding homopolymers, indicating that no graft copolymers (in which $PTHF_x$ would join the PTP backbone at various phosphorus or sulfur sites) had been formed. Switching groups (alkyl groups on the sulfur(VI)) in the copolymer could not be identified, presumably as a consequence of the high molecular weights of the materials (by GPC broad, essentially monomodal peaks were detected with $M_w > 10^5$ and PDI values of 1.5−1.9). Control of $PTHF_x$ block length was attempted by varying factors such as reaction time and temperature. No conclusive relationships were determined, but three polymers with different compositions, $PBATP_{705}-PTHF_{1300}$, $PBATP_{280}-PTHF_{2740}$, and $PBATP_{135}-PTHF_{4925}$, were prepared and identified by ^{1}H NMR and GPC.

Assignment of a block copolymer structure was further supported by the following experiment: first, addition of a CH_2Cl_2 solution of a mechanical blend of $PBATP_{635}$ and $PTHF_{1810}$ to cold hexanes resulted exclusively in the precipitation of $PTHF_{1810}$. In Figure 1 it can be clearly seen that peaks associated with $PBATP_y$ are no longer present in the ^{1}H NMR spectrum of the precipitated product (spectrum B). Under similar experimental conditions, the precipitate formed from solutions of $PBATP_{135}-PTHF_{4925}$ has the same composition as the initial solute. ^{1}H NMR shows (see Figure 2) that the relative ratio of peak integrations (of $PTHF_x$ peaks relative to selected $PBATP_y$ peaks) remains unchanged when comparing the original solute with the precipitate. This behavior is expected for a block copolymer but not for a blend (as shown by the first experiment).

In addition, a dramatic increase in molecular weight was observed when samples of $PMATP_y$ and $PMATP_y-PTHF_x$, synthesized from the same batch of $PCTP_y$ (see Scheme 1), were analyzed by GPC.[24] The GPC (run in THF relative to polystyrene standards) data showed $M_w = 7.0 \times 10^3$ (PDI = 1.5) for $PMATP_y$ and $M_w = 1.5 \times 10^5$ (PDI = 1.9) for $PMATP_y-PTHF_x$. The $PTHF_x$ block of the latter species has much more favorable interactions with solvent than the $PMATP_y$ block, resulting in a large increase in hydrodynamic radius between $PMATP_y$ and $PMATP_y-PTHF_x$. In GPC, molecular weight is related to retention time on the column, which is itself related to hydrodynamic radius. When the hydrodynamic radius of an analyte in a given solvent is different from that of the polystyrene standards, the molecular weights so determined are only approximate.

DSC analysis of $PBATP_y-PTHF_x$ and $PMATP_y-PTHF_x$ showed distinct thermal transitions for the $PATP_y$ and $PTHF_x$ blocks, indicating that the blocks are immiscible and phase separate in the solid state.[25] $PBATP_{705}-PTHF_{1300}$, for example, exhibited a T_g at −70 °C and a T_m at 40 °C due to the $PTHF_{1300}$ block and a T_g at −16 °C due to the $PBATP_{405}$ block. $PMATP_y-PTHF_x$, similarly, exhibited independent thermal transitions for the $PTHF_x$ ($T_g = -79$ °C and $T_m = 34$ °C) and $PMATP_y$ ($T_g = 13$ °C). Note that in a random copolymer, the T_g value would be intermediate to those of the corresponding homopolymers.

Oxygen Diffusion Studies in Polymers. Several factors affect the suitability of a material as a matrix for a pressure-sensitive paint. Most importantly, it must solubilize the dye without compromising its phosphorescent lifetime, and must be sufficiently permeable to oxygen that useful contrast is obtainable in sensor applications. Herein we consider two dyes, PtOEP and $[Ru(dpp)_3]Cl_2$, whose spectroscopic properties in the polymer films under consideration are similar to their properties in common organic solvents.

Although the appearance of the emission spectrum is essentially unchanged in the polymers from that in solution, the emission lifetime of the dye (τ^0) is quite sensitive to the dye's environment. For the rigorous application of eqs 2−5, the dye should exhibit a simple (i.e., single) exponential decay of its luminescence, particularly in the absence of quencher. This is generally not true for ruthenium dyes, which almost always exhibit deviations from simple exponential behavior.[16,26] For $[Ru(dpp)_3]Cl_2$ in $PBATP_{135}-PTHF_{4925}$, the emission decay can be fitted to a sum of two exponential terms. The mean decay lifetime we calculate, $\langle\tau^0\rangle = 6.9\ \mu$s is, however, the same as the unquenched decay lifetime in $PBATP_y$.[15]

The platinum porphyrin dyes in the absence of oxygen, in contrast, do show exponential decays of their phosphorescence intensity in various $PATP_y$ matrixes.[26] For PtOEP, we find simple exponential decays in both $PBATP_y$ and $PBATP_y-PTHF_x$, with lifetimes of 103 and 96 μs, respectively, while the lifetime in freshly

(26) Jayarajah, C. M. Sc. Thesis, University of Toronto, 1998.

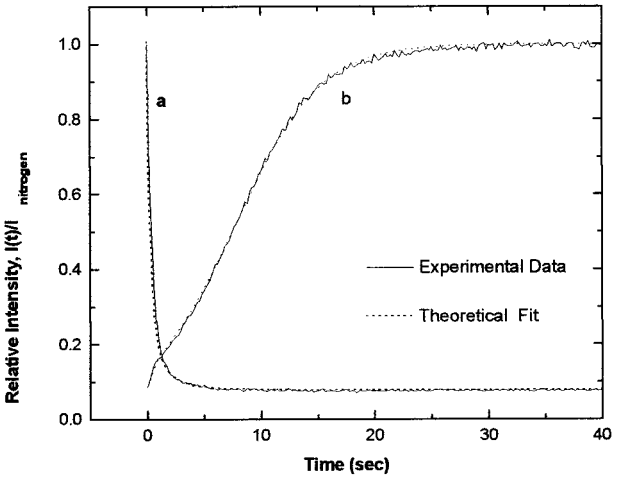

Figure 3. Plot of the luminescent intensity of PtOEP (100 ppm) in a film of copolymer $PBATP_{705}-PTHF_{1300}$ (L = 0.092 mm) on glass as a function of time. Curve a ($D_{O_2} = 9.80 \times 10^{-6}$ cm²·s⁻¹) is obtained from an oxygen sorption experiment, curve b ($D_{O_2} = 9.85 \times 10^{-6}$ cm²·s⁻¹) from an oxygen desorption experiment.

annealed $PTHF_x$ is slightly shorter at 92 μs. These lifetimes were found to be dependent on film age for both $PBATP_y-PTHF_x$ and $PTHF_x$. The emission lifetime in a $PTHF_x$ film aged 10 days drops to 86 μs, and to 75 μs in a film aged 30 days. In a $PBATP_y-PTHF_x$ film aged 3 days, the observed PtOEP emission lifetime was 94 μs. Another example of this sensitivity of τ^0 to a dye's environment concerns the value $\tau^0 = 79$ μs reported for PtOEP−$PBATP_y$ in our initial publication on the system.[15] Upon revisiting this system, it was shown that the shorter lifetime was due to small amounts of residual solvent left in the samples (which were dried in air at room temperature). In the experiments reported herein, all samples were initially air-dried and subsequently heated under vacuum to drive off all solvent. This accounts for the discrepancy between the data reported herein and those reported in ref 15.

Evaluation of the Block Copolymers $PBATP_y-PTHF_x$. The parameters B, D_{O_2}, S_{O_2}, and P_{O_2} were determined for the $PBATP_y-PTHF_x$ block copolymers by measuring the phosphorescence as a function of time, as outlined in the Experimental Section. The time-scan luminescence intensity profiles for PtOEP in $PBATP_{705}-PTHF_{1300}$ are given in Figure 3. Curve a shows the rapid quenching which occurs when the nitrogen-equilibrated film is suddenly exposed to 1 atm of air, and curve b shows the much slower growth in intensity when the air-equilibrated film is exposed to nitrogen. The data from these experiments is fitted to eq 5, using the magnitude of D_{O_2} as the fitting parameter. The parameter B is determined independently from the ratio of the luminescence intensities in the presence of nitrogen and air at equilibrium.

In this way we find $D_{O_2} = 9.80 \times 10^{-6}$ cm²·s⁻¹ for the oxygen sorption measurement and $D_{O_2} = 9.85 \times 10^{-6}$ cm²·s⁻¹ for the desorption measurement. This experiment was carried out ~1 h after removing the sample from the annealing oven. Films of $PBATP_{705}-PTHF_{1300}$, however, become noticeably hazy on standing, and sample age affects the results. The average D_{O_2} value obtained from 12 measurements on three film samples (all aged ~1 h) was $D_{O_2} = (10.9 \pm 0.6) \times 10^{-6}$ cm²·s⁻¹. Substituting D_{O_2} and B into eq 4, a value of $S_{O_2} = 0.8 \pm 0.1 \times 10^{-4}$ M·atm⁻¹ is calculated.

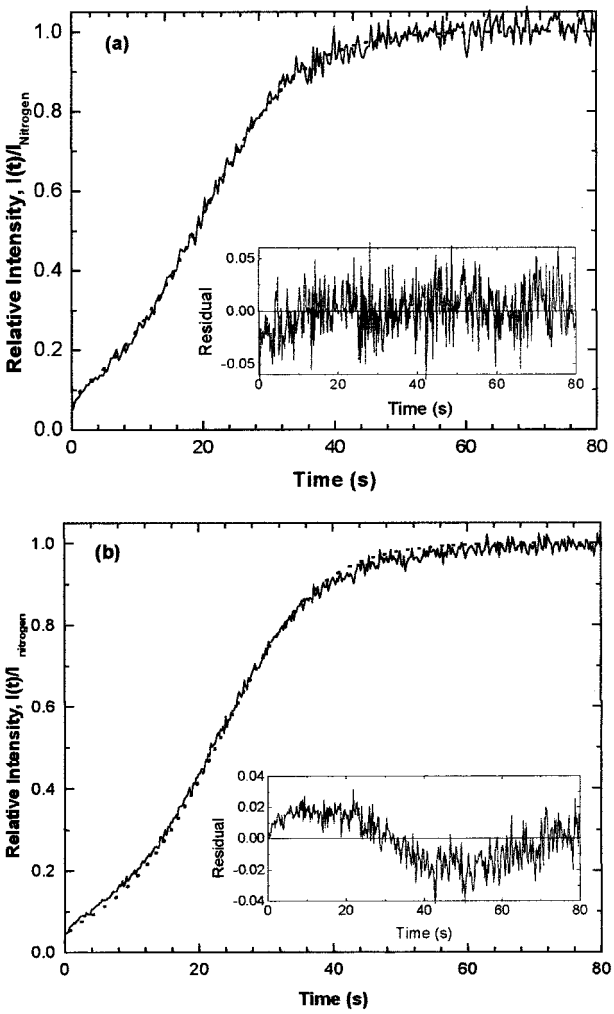

Figure 4. Plot of the luminescent intensity of PtOEP (100 ppm) in a film of copolymer $PBATP_{135}-PTHF_{4925}$ (L = 0.058 mm) on glass as a function of time. Curve a ($D_{O_2} = 1.6 \times 10^{-6}$ cm²·s⁻¹) is obtained from a freshly annealed film, curve b ($D_{O_2} = 1.0 \times 10^{-6}$ cm²·s⁻¹) from a film aged 3 days. The insets are plots of residuals ($I_{expt} - I_{fit}$).

When films of $PBATP_{135}-PTHF_{4925}$ containing PtOEP are examined within 1 h or so of annealing, they give plots strongly resembling those in Figure 3. The simulated and experimental data overlap, and the D_{O_2} values from the sorption and desorption experiments agree to better than 5%. For three films, values of $B = 23.0 \pm 1.0$ and $D_{O_2} = (1.55 \pm 0.07) \times 10^{-6}$ cm²·s⁻¹ were obtained, from which a value of $S_{O_2} = (10.2 \pm 0.5) \times 10^{-4}$ M·atm⁻¹ is calculated. We draw the initial conclusion that the oxygen diffusion coefficient for $PBATP_{135}-PTHF_{4925}$ is a factor of 7 lower than that for $PBATP_{705}-PTHF_{1300}$.

This difference in D_{O_2} values is very important. Examining the desorption curves in Figures 3 and 4, we see that O_2 desorption in $PBATP_{705}-PTHF_{1300}$ requires ~10 s to increase the PtOEP emission intensity to half its final value in a film 0.092 mm thick. In $PBATP_{135}-PTHF_{4925}$, this requires nearly 20 s in a film only 0.052 mm thick. Note that film thicknesses in these experiments were chosen arbitrarily to provide sorption times sufficiently long for data collection. The larger D_{O_2} value for $PBATP_{705}-PTHF_{1300}$ is offset by a lower value for B compared to $PBATP_{135}-PTHF_{4925}$ (12.0 vs 23.0, see Table 1). Since the unquenched lifetimes of

PtOEP are very similar in the two films, the higher B value for $PBATP_{135}-PTHF_{4925}$ means that its lower O_2 diffusion is accompanied by a much higher oxygen solubility! Thus, we see $S_{O_2} = 0.8 \times 10^{-4}$ M·atm^{-1} for $PBATP_{705}-PTHF_{1300}$ and $S_{O_2} = 10.2 \times 10^{-4}$ M·atm^{-1} for $PBATP_{135}-PTHF_{4925}$. The overall permeability of oxygen (P_{O_2}) in the two polymers, however, differs by only a factor of 2 (Table 1).

The aging effects of $PBATP_{135}-PTHF_{4925}$ were examined in greater detail, since the large proportion of $PTHF_x$ makes them much more significant than those observed for $PBATP_{705}-PTHF_{1300}$. Films of $PBATP_{135}-PTHF_{4925}$ are initially clear upon removal from the annealing oven but become hazy and eventually turbid as the $PTHF_{4925}$ phase crystallizes. Time-scan experiments were performed after allowing the samples to age in the dark for 3 days at room temperature. The dye lifetime was found to be essentially unchanged, but the value of B had decreased from 23.0 to 17.4. The time-scan experiments (see Figure 4b) showed evidence for a distribution of diffusion coefficients in the system. For example, if a D_{O_2} value is chosen that gives the best fit at the midpoint of the desorption experiment, the experimental data show a positive deviation from the fit at early times and a negative deviation at late times. From repeated experiments, using simulated curves that gave the best fit to the midpoints of the sorption and desorption curves, we find $D_{O_2} = (1.01 \pm 0.03) \times 10^{-6}$ cm^2·s^{-1}. The values of S_{O_2} and P_{O_2} obtained from this experiment are given in Table 1. In an attempt to appreciate the breadth of the distribution of D values, the early and late parts of the desorption experiment were fitted separately. Intensity profiles that fit the early and late time data were generated, and although they appear very different, the D_{O_2} values differ by only ~20%.

The time-scan experiments on $PBATP_{135}-PTHF_{4925}$ were repeated using $[Ru(dpp)_3]Cl_2$ as the dye. For the samples measured ~1 h after annealing, $B = 1.05 \pm 0.03$ and similar values of D_{O_2} are obtained from the sorption and desorption experiments. For three films, an average value of $D_{O_2} = (2.6 \pm 0.7) \times 10^{-6}$ cm^2·s^{-1} was obtained. This is ~70% larger than the value determined with PtOEP. From the B value, using $\tau^0 = \langle\tau^0\rangle = 6.9$ μs, $S_{O_2} = (3.7 \pm 0.9) \times 10^{-4}$ M·atm^{-1}. The nonexponential decay of the ruthenium dye, however, introduces uncertainty into the calculation of the oxygen solubility. Nevertheless, it appears that $[Ru(dpp)_3]Cl_2$ senses an environment in this copolymer with a lower oxygen solubility and somewhat higher oxygen diffusivity than does PtOEP.

After the films were allowed to age for 3 days in the dark, the time-scan experiments were repeated. These are now very turbid films, but while deviations from a perfect fit of the data to eq 5 were found, they were less pronounced than those with PtOEP. The B value ($B = 1.00 \pm 0.02$) remained identical to that for the fresh film, and the best fit D_{O_2} values for the sorption and desorption experiments were very similar, yielding $D_{O_2} = (1.4 \pm 0.3) \times 10^{-6}$ cm^2·s^{-1}. With the ruthenium dye, the effect of aging was a decrease of ~50% in D_{O_2}, compared to ~35% for PtOEP.

Evaluation of $PTHF_x$ Homopolymer. To understand the aging effects seen for the block copolymers, the aging of $PTHF_x$ was investigated. Time-scan luminescence intensity profiles for PtOEP in $PTHF_x$ are presented in Figure 5. Figure 5a shows the data for a polymer film 1 h after removal from the annealing oven. At this point in time, the film is relatively clear, since little

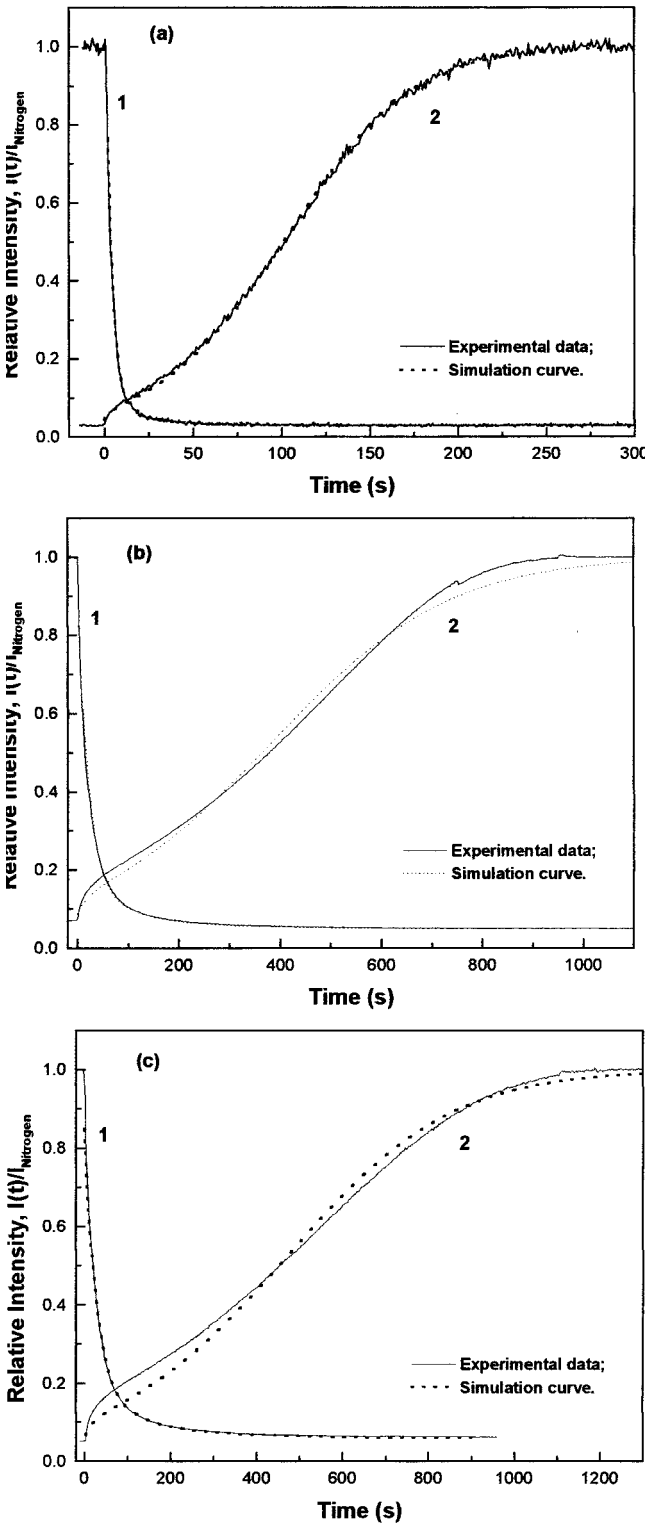

Figure 5. Plot of the luminescent intensity of PtOEP (500 ppm) in a film of $PTHF_x$ ($L = 0.180$ mm) on glass as a function of time. Curve 1 is obtained from an oxygen sorption experiment, and curve 2 from an oxygen desorption experiment. (a) Freshly annealed film, $D_{O_2} = 3.4 \times 10^{-6}$ cm^2·s^{-1}; (b) film aged 10 days, $D_{O_2} = 0.95 \times 10^{-6}$ cm^2·s^{-1}; (c) film aged 30 days, $D_{O_2} = 0.51 \times 10^{-6}$ cm^2·s^{-1}.

crystallization of the polymer has occurred. The D_{O_2} values obtained from the time-scan experiments were very similar and resulted (for a series of experiments) in a value of $D_{O_2} = (3.2 \pm 0.9) \times 10^{-6}$ cm^2·s^{-1}. From the B value (33.5 ± 0.9), using $\tau^0 = 92$

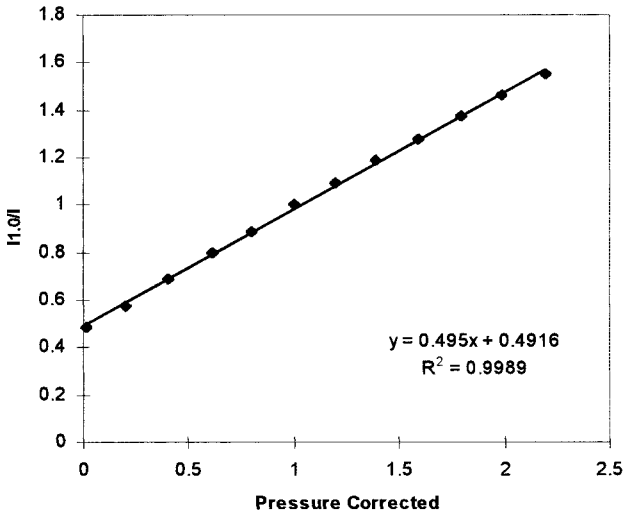

Figure 6. Stern-Volmer-like plot of $I_{1.0}/I$ vs $P/P_{1.0}$ for a film of $PBATP_{280}-PTHF_{2740}$ containing 1000 ppm $[Ru(dpp)_3]Cl_2$, $Q_S = 0.495$, $R^2 = 0.9989$.

μs, we calculate $P_{O_2} = (2.4 \pm 0.2) \times 10^{-12}$ mol·cm^{-1}·s^{-1}·atm^{-1} and $S_{O_2} = (7.4 \pm 2.1) \times 10^{-4}$ M·atm^{-1}.

As the polymer ages, the degree of crystallization increases, and the film becomes more turbid. After aging 30 days in the dark at room temperature, we obtain the time-scan results show in Figure 5c. From these data we obtain $B = 18.9 \pm 1.3$, $\tau^0 = 75$ μs, and $D_{O_2} = (0.68 \pm 0.17) \times 10^{-6}$ cm^2·s^{-1}, all values being significantly smaller than in the freshly annealed sample. From these may be calculated $P_{O_2} = (1.7 \pm 0.1)$ mol·cm^{-1}·s^{-1}·atm^{-1} and $S_{O_2} = (25 \pm 6) \times 10^{-4}$ M·atm^{-1}.

Evaluation $PBATP_y-PTHF_x$ Block Copolymer as Phosphorescent Sensor Matrixes. 1,1,1-Trichloroethane solutions of the block copolymers $PBATP_y-PTHF_x$, containing the dye $[Ru(dpp)_3]Cl_2$, were spray-coated onto aluminum slides primed with a white acrylic base coat.[9] The white base coat reflects light from the back surface and substantially increases the intensity of the detected light. The slides were allowed to age in the dark for at least 16 h prior to running the experiments. They were then placed in a chamber containing air whose pressure was varied incrementally from ~0.3 to 33 psi, and the luminescence intensity (I) was measured. The performance of the phosphorescent sensor matrixes were evaluated from the slopes and linearity of Stern−Volmer-like (SV) plots of $I_{1.0}/I$ vs $P/P_{1.0}$, as per eq 9. As described previously, the slope of this plot, Q_S, is a dimensionless measure of the sensitivity of the dye−polymer combination to quenching by atmospheric oxygen. The plots (e.g., Figure 6) were linear, giving R^2 values in the range of 0.989−0.999. Tests were done to evaluate the effect of $PTHF_x$ chain length on Q_S, and one matrix was further evaluated to determine its photostability and the effect of dye concentration.

Prior to evaluating the effect of $PTHF_x$ chain length on the quenching sensitivity of the block copolymers, the effect of $PTHF_x$ percentage in mechanical blends of $PTHF_x$ and $PBATP_{635}$ was investigated. The quenching sensitivity of $[Ru(dpp)_3]Cl_2$ in films of $PTHF_x$ ($Q_S = 0.37$) was found to be ~30% lower than the sensitivity of that dye in $PBATP_y$ ($Q_S = 0.52$). These Q_S values, and those of blends of the two homopolymers of various composition, have been placed in Table 3. These data show that, regardless of the percentage of $PTHF_x$, the blends all exhibit quenching sensitivities similar to that of $PTHF_x$ itself.

Table 3. Quenching Sensitivity (Q_S) of $PBATP_y/PTHF_x$ Blends as a Function of Blend Composition

wt % $PBATP_{635}$[a]	wt % $PTHF_x$[b]	Q_S
100	0	0.520 ± 0.039
75	25	0.353 ± 0.038
50	50	0.365 ± 0.031
25	75	0.365 ± 0.032
0	100	0.370 ± 0.029

[a] $PBATP_{635}$, $M_w = 3.69 \times 10^5$, PDI = 1.8. [b] $PTHF_x$ $M_w = 8.14 \times 10^4$, PDI = 1.6.

Table 4. Quenching Sensitivity (Q_S) of $[Ru(dpp)_3]Cl_2$ in the Copolymers $PBATP_y-PTHF_x$ as a Function of the Degree of Polymerization of PTHF

polymer	M_w (PDI)	Q_S
$PBATP_{635}$	3.69×10^5 (1.8)	0.519 ± 0.031
$PBATP_{705}-PTHF_{1300}$	3.05×10^5 (1.9)	0.556 ± 0.029
$PBATP_{280}-PTHF_{2740}$	2.61×10^5 (1.5)	0.470 ± 0.031
$PBATP_{135}-PTHF_{4925}$	2.36×10^5 (1.9)	0.495 ± 0.033[a]

[a] The standard deviation in six separate experiments of this sample was found to be 0.495 ± 0.007.

Unlike the blends, the block copolymer matrixes show quenching sensitivities closer to that of $PBATP_y$ than to $PTHF_x$ (see Table 4). For example, $PBATP_{705}-PTHF_{1300}$ has a Q_S (0.56) within experimental error of that of $PBATP_y$. Polymers $PBATP_{280}-PTHF_{2740}$ and $PBATP_{135}-PTHF_{4925}$ have Q_S values (0.50 and 0.47, respectively) somewhat smaller than (but again within experimental error of) that of $PBATP_y$. Overall, the $PTHF_x$ block length appears to have a slight effect on Q_S. The data currently available, however, are insufficient to quantify this effect.

The polymer $PBATP_{135}-PTHF_{4925}$ was chosen for the dye concentration and photostability experiments due to its desirable physical attributes (see Discussion). If Q_S were found to be sensitive to the concentration of dye dispersed in the matrix, this would indicate the formation of dye aggregates, which are fluorescent but have luminescent lifetimes different from that of isolated dye molecules. Such behavior is observed in silicone-based resins, and results in curvature of the SV plots (and thus variation in the values of Q_S). Experiments using $[Ru(dpp)_3]Cl_2$ concentrations varying from 500 to 2500 ppm all resulted in linear plots with Q_S values independent of dye concentration (see Table 5).

There is, thus, no evidence for association of the ruthenium dye in the block copolymer matrixes for this range of dye concentrations. While this experiment is not definitive, it does point to miscibility at the molecular level of the dye in the block copolymer matrix.

Photostability of this dye−matrix combination was evaluated by continuously illuminating the sample and collecting data at a number of times. These data show that emission intensities measured over a 2 h interval do not decrease significantly (see Table 2), indicating that the dye molecules are not significantly photobleached on this time scale.[27] To verify that the sensor matrix does not degrade, Q_S was determined three times during 4 h of

Table 5. Quenching Senitsivity (Q_S) of $[Ru(dpp)_3]Cl_2$ in $PBATP_{135}$–$PTHF_{4925}$ as a Function of Dye Concentration

dye concn (ppm)	Q_S
500	0.486 ± 0.033
1000	0.495 ± 0.029
1500	0.494 ± 0.026
2000	0.488 ± 0.031
2500	0.482 ± 0.034

Table 6. Quenching Sensitivity (Q_S) of $[Ru(dpp)_3]Cl_2$ in $PBATP_{135}$–$PTHF_{4925}$ as a Function of Time

time (h)	Q_S
0	0.491 ± 0.033
3	0.486 ± 0.027
4	0.486 ± 0.024

constant illumination. The SV plots remained linear, and the Q_S values were unaffected within experimental error (see Table 6).

DISCUSSION

Films of $PBATP_y$ have high oxygen permeability, and this polymer is effective at dissolving a number of dyes with long luminescence lifetimes. These are very desirable properties for a PSP matrix material. Unfortunately $PBATP_y$ films are soft and tacky.[9] $PTHF_x$ also has high oxygen permeability, but it is a crystalline polymer that forms brittle films. As the polymer crystallizes, its permeability to oxygen decreases, as does the rate of diffusion of oxygen in the polymer. When these polymers are joined into a block copolymer, one can obtain films with synergistic properties. The block copolymer forms free-standing films that are not tacky and have reasonable mechanical properties. In addition, we find that the block copolymer films have oxygen permeabilities close to those of $PBATP_y$, even in polymers in which the $PTHF_x$ block is much longer than the $PBATP_y$ block.

DSC analysis of the block copolymers in the bulk state revealed thermal transitions corresponding to those of the individual components. This type of behavior is common to block copolymers in which the two blocks are immiscible and form separate microphases in the solid state. If the two polymers were miscible, one would observe a glass transition at a temperature intermediate between those of the two components. One of the transitions found in the block copolymer films is a melting transition of the $PTHF_x$ block. The crystalline domains are the likely source of the mechanical rigidity of the block copolymer films and their surface hardness. Nevertheless, the slow crystallization of these blocks leads to time-dependent gas permeability for the block copolymers. Freshly prepared films are clear. As these films age, they become turbid or hazy, whereas films of $PBATP_y$ remain transparent. As the weight fraction of $PTHF_x$ in the block copolymers is increased, the mechanical characteristics (film rigidity and surface hardness) of the films improve. These are the films with the highest fraction of crystalline polymer, and for films with thicknesses on the order of 0.1–0.3 mm, the most turbid. Fortunately, the oxygen-quenching sensitivity of the matrix, as measured in steady-state Stern–Volmer quenching experiments, is not significantly affected by the block copolymer composition. For this reason, $PBATP_{135}$–$PTHF_{4925}$ (the block copolymer with the highest weight fraction of $PTHF_x$) was chosen as the matrix of choice for the dye concentration and photostability experiments.

Gas permeability (time-scan) experiments were carried out to determine the diffusion coefficients (D_{O_2}), solubilities (S_{O_2}), and permeabilities (P_{O_2}) of oxygen in films of the various polymers. In these experiments, we find that the time scale for the major changes in dye emission intensity for oxygen desorption from the film is much longer than the corresponding time scale for oxygen sorption into the films. Determination of the diffusion coefficients of the films results in sorption and desorption curves in which the time scale of desorption is much longer than that for sorption. This type of difference in response and recovery times has been mentioned many times in the literature about oxygen sensors, and we emphasize here that this behavior is a natural consequence of the oxygen concentration profile generated by diffusion that follows Fick's laws.[17]

In freshly prepared block copolymer films, the intensity vs time plots fit very well to the shape predicted for Fickian diffusion of oxygen into or out of the films, and the D_{O_2} values obtained from both experiments were very close (within 5–10%). One should not interpret the clarity of these films as an indication of polymer miscibility. Based on our DSC measurements, there is no evidence for polymer miscibility, and strong evidence in favor of microphase separation. Film clarity is simply an indication that the sizes of the microdomains are too small to scatter light. Under these circumstances, we think that it is remarkable that we find such good agreement between the results of the time-scan experiments and the predictions of simple Fick's law diffusion in the film. The dyes are not covalently bound to the polymer. They are free to partition between the two different microdomains. Oxygen will also partition between the two domains, and its solubility and diffusivity in the two domains should be different. As a consequence, we anticipated a more complex behavior. Both components of the block copolymer are characterized by high oxygen solubilities and oxygen diffusivities (Table 1), but as the Stern–Volmer experiments show, the block copolymers do not behave like a simple blend of the two homopolymers. Despite the high content of $PTHF_x$ in the block copolymers, the quenching sensitivity is more like that of $PBATP_y$ itself than $PTHF_x$.

As the block copolymer films were allowed to age, they became more turbid. When the time-scan experiments on the aged films were repeated, the signal was noticeably noisier than the signal from experiments carried out on the freshly annealed and transparent films. This effect became more marked with film aging. In addition, the individual time-scan plots for the aged films did not fit as well to the model of Fickian diffusion based upon a single diffusion constant. There were two types of differences from the behavior predicted by the model. First, individual intensity vs time plots exhibited deviations from the model curve (faster diffusion at early times; slower diffusion at later times). Second, there were somewhat larger differences in the D_{O_2} values obtained

(27) Note that while the intensities seem to suggest as much as a 7% loss of intensity (113 counts on the CCD), the error on these measurements (averages of 1600 individual pixel intensities) amounts to 109 counts. There is, thus, no statistically significant decrease in the intensity over the time period in question. We do not suggest these data indicate an absence of photobleaching in this system.

from the oxygen sorption experiments compared to the desorption experiments. While these deviations were not very large, they indicate that changes in the properties of the film toward oxygen diffusion and oxygen permeation have taken place.

Despite these problems, it was still possible to estimate D_{O_2} values by choosing the best fit to the model at the midpoint of the time-scan trace. P_{O_2} values could be calculated from the measured values of B and the unquenched lifetime τ^0. As the data in Table 1 show, aging leads to a decrease in D_{O_2} values, but much smaller changes in P_{O_2} values. For example, with PtOEP in $PBATP_{135}-PTHF_{4925}$, D_{O_2} values decreased by ~65% after 3 days aging at room temperature, whereas P_{O_2} decreased by 25%. With the ruthenium dye, there was also a decrease in D_{O_2}, but hardly any change in P_{O_2}. In addition, the D_{O_2} and P_{O_2} values determined with the two dyes were significantly different. Ordinarily, one might expect the gas permeability properties measured to be independent of the probe, but in the block copolymer samples, one has to take account of the possibility that the dyes are distributed differently between the different domains in the system.

While these turbidity effects proved problematic for the determination of D_{O_2} values, they seemed not to be a problem in the much thinner films used for sensor applications. In sensor applications, thin films are desired to provide response times as short as possible. Much thicker films were used in the time-scan experiments to allow sufficiently long data acquisition times.

In closing, we would like to note two unusual features of our data that remain difficult to explain. First, the D_{O_2} value of $PBATP_{705}-PTHF_{1300}$, determined with PtOEP was found to be almost 1 order of magnitude larger than that of $PBATP_{135}-PTHF_{4925}$. The latter polymer had a correspondingly higher oxygen solubility (S_{O_2}) such that the permeability of oxygen in the two polymers differed by only a factor of 2. Recall that P_{O_2} is calculated via eq 4 from measured values of B and τ^0, whereas P_{O_2} is calculated directly from the shape of the intensity vs time plot in the time-scan experiments. There was excellent reproducibility in both sets of experiments.

The second curious result is found in the comparison of the time-scan and Stern−Volmer experiments. Although the B value of PtOEP in $PBATP_{705}-PTHF_{1300}$ is only half that of $PBATP_{135}-PTHF_{4925}$ (for freshly prepared samples), the Q_S value of $[Ru(dpp)_3]Cl_2$ in the former polymer (0.56) is larger than that of the latter polymer (0.47)! Since $Q_S = B/(1 + B)$, this would not appear to be reasonable. These experiments involve different dyes, and unfortunately, there was not enough of the $PBATP_{705}-PTHF_{1300}$ material to carry out time-scan experiments with both dyes. As a consequence, we are not able to compare B values and Q_S values for the same dye. Nevertheless, this change in behavior is unexpected. We ascribe this occurrence both to aging effects in $PBATP_{135}-PTHF_{4925}$, which are much more dramatic than in $PBATP_{705}-PTHF_{1300}$, and to the possibility that the dyes occupy different sites in the copolymers. While we cannot definitively address this issue, it is worth noting that the blend experiments may tend to suggest that $[Ru(dpp)_3]Cl_2$ is preferentially solvated in the $PTHF_x$ domains. This would account for the quenching sensitivity values being similar to those in $PTHF_x$ even when $PATP_y$ is the dominant component of the blend. The effect of the $PTHF_x$ block length on the magnitude of Q_S is not, however, fully understood.

SUMMARY

We have prepared $PATP_y-PTHF_x$ block copolymers and examined their properties as matrixes for dyes whose excited states serve as oxygen sensors. PtOEP exhibits an exponential decay in $PBATP_y$, $PBATP_{705}-PTHF_{1300}$, and $PBATP_{135}-PTHF_{4925}$ and was used to determine the coefficients of oxygen diffusion and oxygen solubility in the matrixes. These experiments established that D_{O_2} values determined for the block copolymers decreased as a function of time following removal of the films from the oven, where they had been annealed above the melting temperature of the $PTHF_x$ block. For films of $PBATP_{135}-PTHF_{4925}$ with similar thermal histories, but containing different phosphorescent dyes, we calculate somewhat higher D_{O_2} values and lower S_{O_2} values for $[Ru(dpp)_3]Cl_2$ than for PtOEP.

The block copolymers $PBATP_y-PTHF_x$ with $[Ru(dpp)_3]Cl_2$ as the dye have excellent properties for air pressure sensor applications. They exhibit good quenching sensitivity and linear Stern−Volmer-like plots when the emission intensity is determined at different air pressures. Further, the block copolymers form free-standing films with much better mechanical properties (i.e., nontacky films) than $PBATP_y$, and have Q_S values for $[Ru(dpp)_3]Cl_2$ much higher than those in $PBATP_y/PTHF_x$ blends. Work aimed at using these and related polymers for specific sensor applications is currently underway.

ACKNOWLEDGMENT

The authors thank Materials and Manufacturing Ontario (MMO) and NSERC Canada for their support of this research.

Received for review August 24, 1999. Accepted January 3, 2000.

AC9909610